

Cite this: *Analyst*, 2020, **145**, 4069

## Recent advances in nanomaterial-enhanced enzyme-linked immunosorbent assays

Lu Gao,<sup>a</sup> Qianfan Yang,<sup>a</sup>  \*<sup>a</sup> Peng Wu  <sup>a</sup> and Feng Li  \*<sup>a,b</sup>

Despite serving as a gold standard for protein analysis, the classic enzyme-linked immunosorbent assay (ELISA) is currently challenged by the ever-increasing needs of sensitivity and simplicity. Towards the ongoing needs, recent advances in nanomaterials have offered numerous promising tools for enhancing the performance and broadening the applicability of ELISA. In this review, we highlight nanomaterial-enabled strategies that drastically improve the assay performance without significantly altering the classic ELISA format. Particular attention will be focused on the functional roles of nanomaterials as novel readout systems in ELISA, including those serving as substrate-alternatives, enzyme-alternatives, and non-enzymatic signal amplifiers.

Received 27th March 2020,  
Accepted 3rd May 2020

DOI: 10.1039/d0an00597e

rsc.li/analyst

### 1. Introduction

Since first introduced in 1971,<sup>1</sup> enzyme-linked immunosorbent assay (ELISA) has been widely accepted as a gold standard for protein detection and quantification in disease

diagnosis,<sup>2</sup> food safety testing,<sup>3</sup> and environmental monitoring.<sup>4</sup> A typical ELISA assay involves four main steps,<sup>5</sup> including (1) immobilization of a target protein on a solid support either through a capture antibody or nonspecific adsorption, (2) target recognition using detection antibodies, (3) signal amplification *via* an enzymatic reaction, and (4) signal readout generated by a chromogenic or fluorogenic substrate. Combining antibody-mediated target recognition and enzyme-driven signal transduction, ELISA allows the specific detection of as low as picomolar level proteins.

<sup>a</sup>Key laboratory of Green Chemistry & Technology of Ministry of Education, College of Chemistry, Analytical & Testing Center, Sichuan University, 29 Wangjiang Road, Chengdu, Sichuan, China, 610064. E-mail: fli@brocku.ca

<sup>b</sup>Department of Chemistry, Brock University, 1812 Sir Isaac Brock Way, St. Catharines, Ontario, Canada, L3S 3A1



Lu Gao

Lu Gao received her B.Sc. degree in chemical engineering and technology from Northeast Forestry University in 2018. She is currently working towards her PhD degree in Analytical Chemistry at Sichuan University under the direction of Professor Feng Li. Her current research is focused on developing novel DNA nanostructures and devices for sensitive protein detection and disease diagnosis.



Qianfan Yang

Qianfan Yang received his Ph.D. (2010) at Institute of Chemistry, Chinese Academy of Science (ICCAS). During his research career from 2005 to 2015 at ICCAS, his research was mainly on novel DNA structural probes and their applications. From 2013 to 2014, he joined Professor Jorge Torres' lab at University of California, Los Angeles (USA) as a visiting scholar to study on high-throughput screening of genes involved in cell mitosis. Then he came to College of Chemistry, Sichuan University (China) as an associate Professor in 2015. His current research interests are focused on developing new DNA-based analytical techniques for biomarkers.

Although sufficient for routine protein analysis, better diagnostic and/or prognostic uses of ELISA demand improved sensitivity.<sup>6,7</sup> For example, post-surgical monitoring prostate specific antigen (PSA) at femtomolar level has shown better predictive values for the reoccurrence of prostate cancer.<sup>8</sup> As such, many research efforts have to improve the sensitivity of ELISA, revealing at least two viable solutions. The first solution involves the modification or replacement of conventional enzyme-based signal readout with more sensitive ones. A classic example is immuno-PCR,<sup>9</sup> where a synthetic DNA strand and polymerase chain reaction (PCR) are used to facilitate the signal amplification for ELISA. The second solution focuses on converting the classic microplate-based ELISA into digital ELISA,<sup>10</sup> where each assay is aliquoted into thousands of microwells or droplets and thus generates digital signal readouts. Besides sensitivity, advances in novel immunoassays are also driven by their applicability and user-friendship in infrastructure-limited settings. Miniaturization of ELISA into rapid, portable, point-of-care tests (POCT) represents a new trend towards personalized medical care and disease diagnosis in resource-limited countries or regions.<sup>11,12</sup> Along with this trend, numerous efforts have been made to develop novel readout systems for ELISA, which are both sensitive and user-friendly.<sup>13,14</sup>

Towards the ongoing need of improved sensitivity and/or user-friendship, diverse biohybrid nanomaterials have been designed and employed as novel readouts in immunoassays.<sup>15</sup> Immunoassays harnessing unique optical, electrochemical, catalytic, or structural properties of nanomaterials have been reviewed extensively in the past years.<sup>16–20</sup> The previous reviews discussed nanomaterial-enhanced immunoassays based primarily on the types of materials or signal readouts. The functional roles of nanomaterials in immunoassays have not been reviewed extensively. Herein, we focus this review on

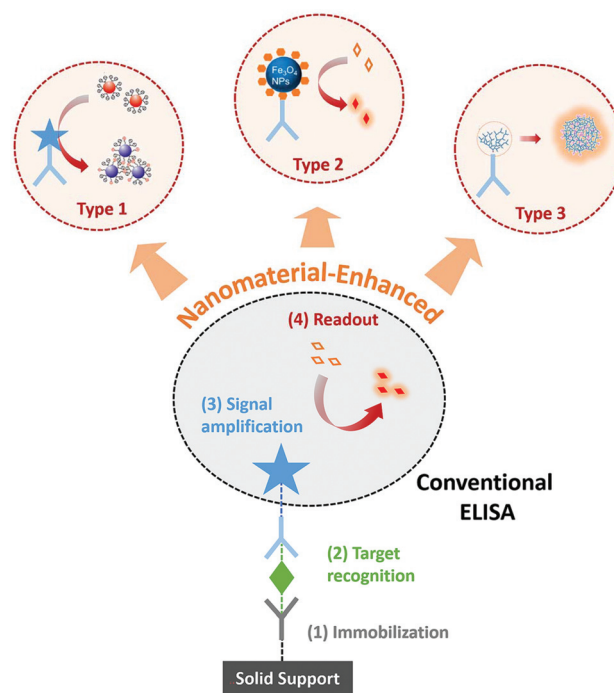


**Fig. 1** Schematic diagram showing the enhancement of conventional ELISA by using nanomaterials as substrate-alternatives (Type 1), enzyme-alternatives (Type 2), or enzyme-free amplifiers (Type 3).

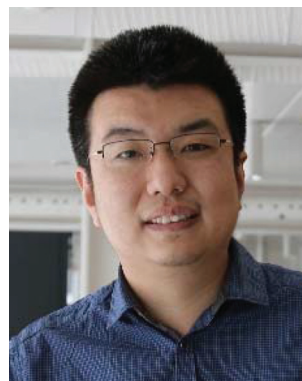
their functional roles as novel signal readouts for enhancing ELISA, including those serve as substrate-alternatives, enzyme-alternatives, or enzyme-free amplifiers (Fig. 1). This review will help guide the design and translation of novel nanomaterial-based readout systems for improving ELISA with minimal alterations of the classic assay format.



**Peng Wu**

*Peng Wu is a professor of analytical chemistry at Sichuan University, China. He received his BS and MSc both from Sichuan University in 2003 and 2006, respectively, and PhD in analytical chemistry from Nankai University in 2011. He was a postdoctoral fellow in Nanjing University between 2013 and 2015. He has published over 70 papers in peer-reviewed journals. He was the recipient of the Chinese National Science Fund*

*for Excellent Young Scholars of China in 2015. Currently, his research interests focus on the development of new optosensing and bioanalytical methods for disease-related biomolecules/pathogens based on room-temperature phosphorescence and oxygen photosensitization.*



**Feng Li**

*Feng Li is currently a Professor of Chemistry at Sichuan University (Chengdu, China). He received his Ph.D. in Analytical Chemistry from University of Alberta (Canada) in 2013. Before joining Sichuan University, he was appointed as an Assistant Professor of Chemistry at Brock University (St Catharines, Canada) in 2014 and was promoted to Associate Professor in 2019. His research is at the interface of analytical chemistry*

*and DNA nanotechnology, with a focus on developing novel analytical devices/assays for measuring disease biomarkers and creating new DNA nanodevices and DNA nanotechnology for diagnostic and medical applications.*

## 2. Immunoassays using nanomaterials as substrates

Detection signals of classic ELISA are generated through the enzymatic conversion of chromogenic or fluorogenic substrates, such as 3,3',5,5'-tetramethylbenzidine (TMB), 2,2'-azino-bis-(3-ethylbenzthiazoline-6-sulfonic acid) (ABTS) and *o*-Phenylenediamine (OPD). One limiting factor to the sensitivity of ELISA is the low extinction coefficients of these small molecular substrates (at  $10^4 \text{ M}^{-1} \text{ cm}^{-1}$  level).<sup>21,22</sup> On the other hand, extinction coefficients for plasmonic nanoparticles, such as gold nanoparticles (AuNPs), can reach as high as  $10^8$  to  $10^9 \text{ M}^{-1} \text{ cm}^{-1}$  because of the unique localized surface plasmon resonance (LSPR).<sup>23</sup> According to Beer-Lambert law, the solution absorbance is linearly correlated to the extinction coefficient. The higher extinction coefficient would be beneficial for higher detection sensitivity. As such, replacing commonly used small molecular substrates with plasmonic nanoparticles can lead to a drastic improvement of the conventional ELISA in terms of the assay sensitivity. Thus inspired, numerous strategies have been explored to integrate ELISA with plasmonic readouts.<sup>24–27</sup> These types of novel immunoassays are generally accepted as plasmonic ELISA.

The idea of plasmonic ELISA was first introduced by Stevens and coworkers in 2012 (Fig. 2A).<sup>28</sup> The assay workflow is adapted from ELISA, except that plasmonic AuNPs were used instead of conventional small molecular substrates. In the absence of the analyte, gold ions were rapidly reduced by hydrogen peroxide ( $\text{H}_2\text{O}_2$ ) to form quasi-spherical, non-aggregated AuNPs, and the color of the reaction solution is red. In the presence of the target protein, however, catalase is introduced to the reaction mixture through the target-specific immunocomplexes. As catalase consumes  $\text{H}_2\text{O}_2$ , the newly formed AuNPs are of ill-defined morphology with aggregates. The surface plasmon resonance is caused by the collective oscillation of the conduction electrons across the nanoparticle. Therefore, the aggregates of AuNPs results in significant red-shifting (from  $\sim 520$  to  $\sim 650 \text{ nm}$ ) due to the interparticle plasmon coupling, leading to a sharp red-to-blue color transition. Using this principle, the plasmonic ELISA enabled ultra-sensitive detection of PSA and HIV-1 capsid antigen p24 in serum samples with LODs as low as  $1 \times 10^{-18} \text{ g mL}^{-1}$ . In addition to catalase, other enzymes, such as glucose oxidase (GOx),<sup>29</sup> alcohol dehydrogenase,<sup>30</sup> have been used to catalyze the growth of metal nanoparticles to achieve ultra-sensitive naked-eye detection (Table 1).

Besides controlling the growth of plasmonic nanoparticles, directly inducing aggregations of metal nanoparticles is another commonly used strategy to enhance the sensitivity of ELISA. For example, Chen and coworkers<sup>31</sup> designed a novel plasmonic ELISA (Fig. 2B), where acetylcholinesterase (AChE) was used to produce thiocholine. Thiocholine induced the subsequent aggregation of citrate-capped AuNPs and thus resulting in a strong red-to-purple color transition. This method allows the visual detection of enterovirus 71 with a



**Fig. 2** Immunoassays using nanomaterials as substrate-alternatives. (A) Schematic diagram of the plasmonic ELISA by the growth of plasmonic nanoparticles and the comparison to the conventional one. In conventional colorimetric ELISA (left), enzymatic biocatalysis generates a coloured compound. While in plasmonic ELISA (right) the biocatalytic cycle of the enzyme generates coloured nanoparticle solutions of characteristic tonality. Reprinted from ref. 28, Copyright, 2012, Springer Nature. (B) Schematic diagram of the ultra-sensitive visual Immunoassay based on the direct aggregations of AuNPs. Reprinted from ref. 31, Copyright, 2013, WILEY-VCH Verlag GmbH & Co. KGaA, Weinheim. (C) Schematic diagram of the multicolour plasmonic ELISA based on the size changes of AuNRs. Reprinted from ref. 40, Copyright, 2014, American Chemical Society. (D) Schematic diagram of the ultra-sensitive immunoassay based on polymeric nanoparticles. Reprinted from ref. 43, Copyright, 2017, Springer Nature.

LOD ( $\sim 10^4$  copies per mL) comparable to that obtained by quantitative PCR. Strategies involving aggregation of plasmonic nanoparticles can be easily adapted into the currently available ELISA platforms and have been successively applied to



**Table 1** Recent advances in nanomaterial-enhanced enzyme-linked immunosorbent assays

The role of nanomaterials	Target protein	Detection limit	Readout	Ref.
Substrate alternatives	Prostate specific antigen (PSA) and HIV-1 capsid antigen p24	1 ag mL <sup>-1</sup>	Colorimetric	28
	PSA	3.1 fg mL <sup>-1</sup>	Colorimetric	29
	Hepatitis B surface antigen and $\alpha$ -fetoprotein	1 pg mL <sup>-1</sup>	Colorimetric	30
	PSA	3 fg mL <sup>-1</sup>	Colorimetric	38
	Alpha fetal protein	0.2 ng mL <sup>-1</sup>	Colorimetric	24
	Enterovirus 71	10 <sup>4</sup> copies per mL	Colorimetric	31
	<i>Treponema pallidum</i> antibodies	1 pg mL <sup>-1</sup>	Colorimetric	32
	Rabbit antihuman IgG; mycoplasma; pneumonia	2 ng mL <sup>-1</sup>	Colorimetric	33
	Human IgG	1 ng mL <sup>-1</sup>	Colorimetric	40
	<i>E. coli</i> O157:H7	50 CFU mL <sup>-1</sup>	Colorimetric	27
	PSA	75 pg mL <sup>-1</sup>	Colorimetric	41
	Aflatoxin B <sub>1</sub> (AFB <sub>1</sub> )	12.5 pg mL <sup>-1</sup>	Colorimetric	39
	HIV antigen	3 fg mL <sup>-1</sup>	Colorimetric	42
	Enzyme alternatives	Hepatitis B virus surface antigen	Not reported	Colorimetric
Mouse interleukin 2 (IL-2)		Not reported	Colorimetric	44
Ebola virus		1 ng mL <sup>-1</sup>	Colorimetric	48
PSA		31 fg mL <sup>-1</sup>	Colorimetric	53
C-Reactive protein (CRP)		0.67 pg mL <sup>-1</sup>	Fluorescent	54
HIV-1 capsid antigen p24		0.8 pg mL <sup>-1</sup>	Colorimetric	55
CEA		9 pg mL <sup>-1</sup>	Colorimetric	56
Apolipoprotein A1 (ApoA1)		20 pg mL <sup>-1</sup>	Colorimetric	57
Nanomaterials as nanocarriers	PSA	32 fg mL <sup>-1</sup>	Fluorescent	65
	AFP	0.74 ng mL <sup>-1</sup>	Fluorescent	68
	PSA	30 amol L <sup>-1</sup>	Grayscale	70
	Rabbit IgG, <i>Salmonella</i> , <i>Listeria</i> , and <i>E. coli</i> O157	30 amol L <sup>-1</sup>	Colorimetric	71
	HIV-1 gp41 antigen	0.1 ng mL <sup>-1</sup>	Colorimetric	72
DNA nanotechnology	Cancerous exosomes	2.1 $\times$ 10 <sup>4</sup> mL <sup>-1</sup>	Electrochemical	73
	Golgi protein 73 (GP73)	15 pg mL <sup>-1</sup>	Electrochemical	74
	immunoglobulin G (IgG)	2.8 pg mL <sup>-1</sup>	Electrochemical	84
	PSA	40 pg mL <sup>-1</sup>	Fluorescent	84
	Cytokine	<1 ng mL <sup>-1</sup>	Fluorescent	93
	HeLa cells	4400 cells per mL	Fluorescent	98

the detection of various targets, including *Treponema pallidum* antibodies,<sup>32</sup> mycoplasma,<sup>33</sup> and HCV.<sup>34</sup>

As LSPR are highly shape- and size-dependent, plasmonic ELISA with multicolored readout have also been achieved by inducing changes in the shape and/or size of plasmonic nanomaterials through etching or deposition.<sup>35–39</sup> For example, Tang and coworkers<sup>40</sup> have developed an ultra-sensitive plasmonic ELISA based on the size changes of gold nanorods (AuNRs) (Fig. 2C). In this assay, ALP was utilized to catalyze the hydrolysis of ascorbic acid 2-phosphate to produce ascorbic acid, which is capable of reducing silver ion to metallic silver. The metal silver then deposited on AuNRs, resulting in a rainbow-like color transition from red, to orange, to yellow, and finally to green. The multicolour transition has also been achieved by etching the anisotropic AuNRs. For example, Lin and coworkers<sup>41</sup> recently developed a multicolour plasmonic ELISA by using TMB to etch AuNRs, allowing the visual detection of carcinoembryonic antigen (CEA) in human serum with a LOD of 2.5 ng mL<sup>-1</sup>.<sup>42</sup> Comparing with monochromatic intensity changes, the multicolour transition is an ideal readout for naked-eye detection and quantification in POCT settings.

In addition to plasmonic nanoparticles, polymeric nanoparticles have also been introduced as substrate alternatives to

conventional ELISA. For example, Gao and coworkers<sup>42</sup> developed an ultra-sensitive immunoassay by combining the polymerization of dopamine with horseradish peroxidase (HRP)-based conventional ELISA in 2017 (Fig. 2D). In the system, HRP catalyzes the localized deposition of polydopamine to form the polydopamine layer, and then the polydopamine layer accumulates more HRP enzymes in turn, which leads to a much stronger color transition. Using this principle, as low as 3 fg mL<sup>-1</sup> of HIV antigen could be detected in blood samples, which is over 1000-fold more sensitive than the conventional ELISA.

The uses of plasmonic or polymeric nanoparticles as substrate alternatives in ELISA allows the improvement of both sensitivity and user-friendship without significantly altering the assay format. Such strategies can be employed directly as “add-on” units to current ELISA platforms, which may help reduce the cost and infrastructural barriers and accelerate their uses in real-world applications.

### 3. Immunoassays using nanozymes

Enzyme is a core component in ELISA to transduce and amplify the specific affinity recognition of target proteins into

## Analyst

sensitive detectable signals. Despite the high catalytic efficiency, commonly used enzymes, such as HRP, ALP, and GOx, are proteins in their chemical nature and thus are susceptible to environmental influences (*e.g.*, pH or temperature). The massive production of such enzymes is also tedious and expensive. As such, nanomaterials have also been investigated as chemical alternatives of naturally existing enzymes to improve the assay robustness and reduce the cost of ELISA.<sup>43–45</sup> These enzyme-like nanomaterials capable of catalyzing chromogenic or fluorogenic reactions in aqueous solutions are generally known as nanozymes.<sup>46</sup>

The enzyme-like nanozyme was first discovered by Yan and coworkers in 2007,<sup>47</sup> where Fe<sub>3</sub>O<sub>4</sub> magnetite nanoparticles (Fe<sub>3</sub>O<sub>4</sub> MNPs) were found to possess intrinsic catalytic activity similar to natural peroxidase (Fig. 3A). Comparing with HRP, Fe<sub>3</sub>O<sub>4</sub> MNPs have shown higher affinity and faster catalytic rate to the substrate TMB, and are more tolerant to environmental changes. This nanozyme was further integrated into a standard ELISA method as an enzyme-alternative to detect hepatitis B virus surface antigen preS1. The same nanozyme was also integrated by the same lab to an immunochromatographic strip, which allows the visual detection of glycoprotein of Ebola virus with a LOD as low as 1 ng mL<sup>-1</sup>.<sup>48</sup> Remarkably, this method is ~100 times more sensitive than the conventional lateral flow strips operated by ELISA. Following these pioneering works, many nanozymes with diverse chemical compositions have been discovered, including cobalt-based,<sup>49</sup> platinum-based,<sup>50</sup> copper-based,<sup>51</sup> and manganese-based,<sup>52</sup> the most of which have been successfully integrated into ELISA assays for ultrasensitive protein detection.<sup>53–57</sup>

Despite the exciting advancement of nanozymes in recent years, their wide applications to immunoassays remain limited by several challenges.<sup>58</sup> For example, unlike natural enzymes with well-defined binding pockets, nanozymes do not contain specific substrate-binding sites and thus are generally lack of substrate-specificity. To address this issue, Liu and coworkers<sup>59</sup> have successfully created substrate (TMB and ABTS) recognition sites on Fe<sub>3</sub>O<sub>4</sub> MNPs using molecular imprinting technology (Fig. 3B). It was found that the imprinted material not only improved the specificity to TMB by nearly 100-times, but also improved the catalytic activity. This study points a possible solution to improve the catalytic specificity of nanozymes, which will expand the application of nanozymes in ELISA.<sup>60</sup>

Another challenge for using nanozymes is their poor catalytic activities at neutral pH. For most nanozymes, their optimal catalytic activities are achieved at acidic conditions rather than physiological pH ranges. Liu and coworkers<sup>61</sup> recently addressed this pH limitation by using Mn(II) as a mediator (Fig. 3C). It was established on the previous observation that the inhibition of the catalytic activity of nanozymes was related to the difficulty of the oxidation of the substrate TMB in neutral conditions.<sup>62</sup> When Mn(II) is added to the reaction, it can be photooxidized to Mn(III) by the nanozymes under neutral conditions. Mn(III) then oxidizes TMB to generate the colorless-to-blue transition. Once integrated to ELISA,

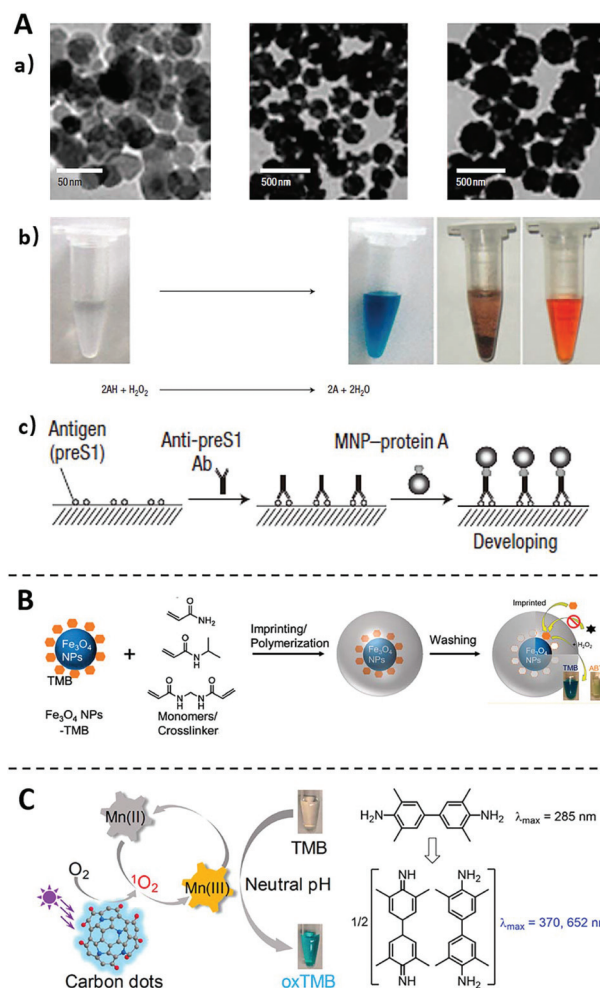


**Fig. 3** Immunoassays using nanozymes (A) and the method for improving nanozyme properties (B and C). (A) TEM images of nanozyme Fe<sub>3</sub>O<sub>4</sub> MNPs, and the Fe<sub>3</sub>O<sub>4</sub> MNPs catalyse oxidation of various peroxidase substrates in the presence of H<sub>2</sub>O<sub>2</sub> to produce different colour reactions. Scheme of the Immunoassay based on the catalysis of Fe<sub>3</sub>O<sub>4</sub> MNPs. Reprinted from ref. 47, Copyright, 2007, Springer Nature. (B) Schematic diagram of imprinting TMB on Fe<sub>3</sub>O<sub>4</sub> NPs to improve their substrate-specificity. Reprinted from ref. 59, Copyright, 2017, American Chemical Society. (C) Schematic diagram of expanding the pH limitation of Carbon dots nanozyme by using Mn(II) as a mediator. Reprinted from ref. 61, Copyright, 2019, American Chemical Society.

nanozymes of extended workable pH range will further improve the assay robustness against environmental factors and thus expand their applicability to POCT and field-based tests.

#### 4. Immunoassays using nanomaterials as non-enzymatic signal amplifiers

While the enhancement of enzymatic reactions by nanomaterials has proven to be an effective solution to improve the

sensitivity and user-friendliness of ELISA, the assay performance may still be limited by the choice of either enzymes (in the case of substrate alternatives) or substrates (in the case of nanozymes). As such, many research efforts have also been emphasized on the development of non-enzymatic signal amplifiers that are compatible with ELISA. Despite no enzymatic reaction is involved, similar operational protocols are applied and newly developed signal amplifiers can be adapted with low technological barriers.<sup>63–68</sup> Nanomaterials have been used exclusively to fulfill this goal, as they may either serve as nanocarriers capable of releasing hundreds to thousands of signal reporters all at once or be programmed into unique DNA nanostructures to amplify optical or electrochemical signals.

#### 4.1 Non-enzymatic signal amplifiers using nanomaterials as nanocarriers

One of the most frequently adopted mechanisms for designing non-enzymatic signal amplifiers for ELISA is to use nanomaterials as nanocarriers that can accommodate and release large amounts of signal reporters.<sup>69</sup> One classical example of such is the biobarcode assay introduced by Mirkin and co-workers in 2003 (Fig. 4A),<sup>70</sup> where detection antibody and hundreds of DNA barcodes were conjugated onto the same AuNP. Using this nanobarcode, the detection of trace amounts of target protein is translated into the detection of large numbers of DNA barcodes. When combined with PCR, the LOD of this biobarcode assay reached as low as 3 aM. The clinical usefulness of this assay was further demonstrated by monitoring the level of PSA for patients undergone radical prostatectomy.<sup>8</sup> Because of the ultrahigh sensitivity, this assay redefined the undetectable level of PSA and thus effectively improve the predictive value of serum PSA for prostate cancer recurrence.

Besides surfaces of nanomaterials, signal reporters can also be encapsulated inside, which will be released during the detection step. Abbas and coworkers developed a liposome-assisted plasmonic ELISA capable of visual detection of specific antibody with a LOD of 6.7 aM (Fig. 4B).<sup>71</sup> In this assay, large amounts of cysteine molecules were loaded into a single liposome. In the presence of the target, the liposome was captured through a detection antibody and then hydrolyzed to release cysteines those can induce the rapid aggregation of AuNPs. Through this non-enzymatic amplification mechanism, this assay improves the sensitivity of conventional ELISA by 6 orders of magnitude. This assay has also been successfully applied to the detection of pathogens, such as *Salmonella*, *Listeria*, and *E. coli* O157.<sup>71</sup>

The chemical composition of nanoparticles can also be used as signal amplifiers for designing ELISA with non-enzymatic readouts. For example, Jiang and coworkers have successfully harnessed copper monoxide nanoparticles (CuO NPs) as signal amplifiers for ultrasensitive protein analysis (Fig. 4C).<sup>72</sup> As Cu(II) is the main chemical composition of CuO NPs, millions of Cu(II) can be released upon acid hydrolysis. Cu(II) is then reduced to Cu(I) in the presence of sodium ascorbate, which accelerates a click reaction between alkyne-modified

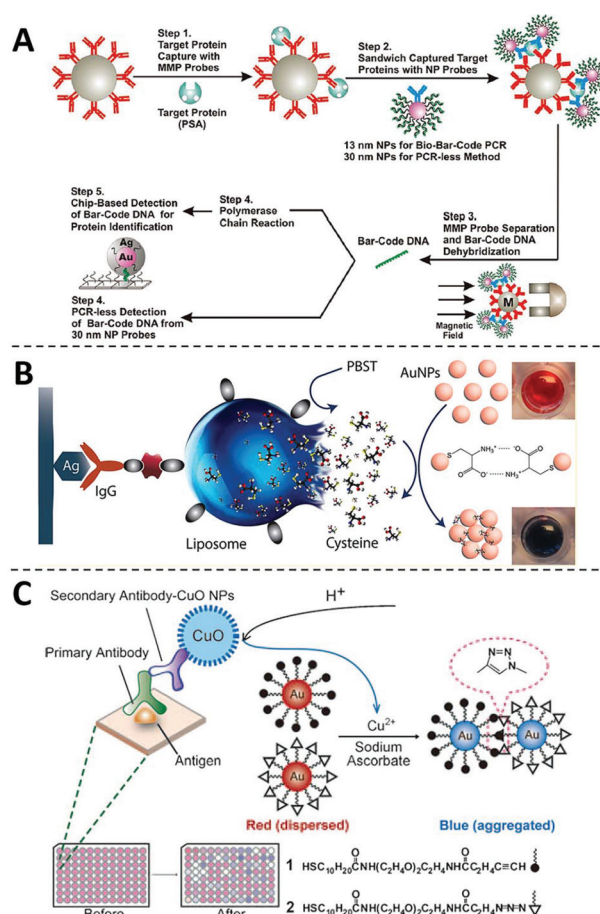


**Fig. 4** The non-enzymatic signal amplifiers using nanomaterials as nanocarriers. (A) Schematic diagram of the probe design, preparation and PSA detection of the biobarcode assay, in which the detection of trace amounts of target protein is translated into the detection of large numbers of DNA barcodes. Reprinted from ref. 70, Copyright, 2003, Springer Nature. (B) Schematic diagram of the liposome-assisted plasmonic ELISA, in which liposomes can load large amounts of cysteine to amplify the detection signals. Reprinted from ref. 71, Copyright, 2015, American Chemical Society. (C) Schematic diagram of the immunoassay based on CuO-labeled antibody and click chemistry. Reprinted from ref. 72, Copyright, 2011, WILEY-VCH Verlag GmbH & Co. KGaA, Weinheim.

fied AuNPs and azid-modified AuNPs and induces their aggregation. This method enabled rapid and equipment-free detection of HIV antibodies, showing its potential to be used as a POCT diagnostic test.

#### 4.2 Non-enzymatic signal amplifiers using DNA nanotechnology

Beyond their roles as nanocarriers, nanomaterials can also be programmed into rationally designed structures or reaction networks for signal amplification. Particularly, recent advances in DNA nanotechnology offer numerous structural and dynamic approaches enabling programmable signal amplification for ELISA.<sup>73–75</sup>

Since first introduced by Seeman and coworkers in 1982,<sup>76</sup> numerous DNA nanostructures and dynamic devices have



been created and found diverse applications in sensing, drug delivery, and biocomputing.<sup>77–82</sup> When integrated with an ELISA protocol and electrochemistry for protein analysis, Fan and coworkers found that the three-dimensional (3D) DNA tetrahedron could effectively control the spatial distribution of antibodies on the electrode and thus effectively eliminate entanglement and masking between adjacent probes (Fig. 5A).<sup>83</sup> As a result, target proteins could be captured with much higher efficiency and the assay sensitivity was much improved with a low LOD of  $2.8 \text{ pg mL}^{-1}$ . Inspired by this work, the DNA tetrahedra and other 3D DNA nanostructures,

such as DNA nanostars, have also been explored to enhance immunoassays.<sup>84–87</sup>

DNA nanotechnology also offers a series of dynamic DNA reactions capable of signal amplification in an isothermal and enzyme-free manner.<sup>88–91</sup> Because of the ability for *in situ* signal amplification, hybridization chain reaction (HCR) has emerged as one of the most widely used DNA amplifiers for protein analysis and imaging.<sup>92</sup> The integration of HCR with ELISA was first explored by Love and coworkers in 2011, where an HCR initiator was conjugated to the detection antibody (Fig. 5B).<sup>93</sup> Once captured by the target protein through the sandwiched binding complex, the initiator triggers the subsequent hybridization of two fluorescently labeled DNA hairpin probes. A long HCR product is then created containing hundreds to thousands of fluorophores. This technology, termed immuno-HCR, allows the quantification of multiple cytokines from human peripheral blood mononuclear cells with LODs at sub-pM levels. Using a similar design, Luo and coworkers further developed a multiplexed immuno-HCR for the simultaneous detection/imaging of multiple protein markers in clinical samples and cells.<sup>94</sup> Immuno-HCR have also been successfully designed for the ultra-sensitive detection of IgG,<sup>95</sup> CEA,<sup>96</sup> and matrix metalloproteinase-7<sup>97</sup> through electrochemical signal readouts.

In addition to linear DNA structures, dendrimeric DNA structures created by hyperbranched HCR reactions have also been integrated with ELISA as non-enzymatic signal amplifiers.<sup>99–102</sup> For example, Liu and coworkers developed a DNA dendrimer-streptavidin nanocomplex *via* a nonlinear HCR reaction (Fig. 5C).<sup>98</sup> This dendrimeric DNA nanostructure was further intercalated with large numbers of SYBR Green I dye and thus significantly amplified fluorescent signals. By integrating this fluorescent DNA dendrimer with ELISA, this assay can detect HeLa cells with a detection limit of  $4.4 \times 10^3$  cells per mL.

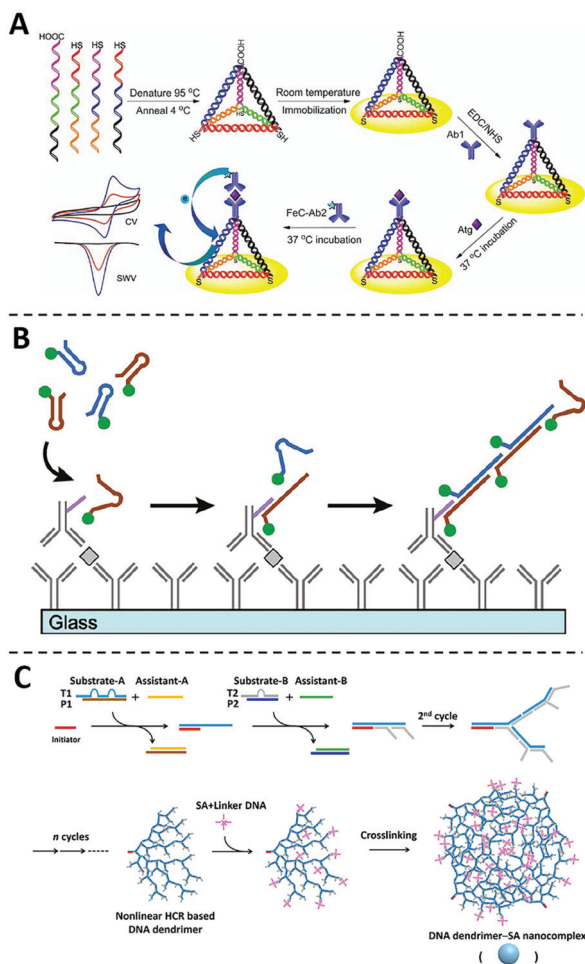


**Fig. 5** The non-enzymatic signal amplifiers using DNA nanotechnology. (A) Schematic diagram of the sandwich immunoassay using the DNA tetrahedron modified Au electrode, in which entanglement and masking between adjacent probes can be effectively eliminated and target proteins could be captured with much higher efficiency. Reprinted from ref. 83, Copyright, 2014, Springer Nature. (B) Schematic diagram of the immuno-HCR, in which the target recognition can trigger the subsequent formation of long HCR products containing hundreds to thousands of fluorophores. Reprinted from ref. 93, Copyright, 2011, American Chemical Society. (C) Schematic diagram of the formation of DNA dendrimer-SA nanocomplex *via* a nonlinear HCR reaction, which can be integrated with conventional ELISA to amplify detection signals. Reprinted from ref. 98, Copyright, 2017, American Chemical Society.

## 5. Conclusion and perspectives

Over the past years, techniques for protein detection and quantification have been driven by the ever-increasing needs of ultra-high sensitivity and assay simplicity.<sup>11–14</sup> Advances in nanotechnology have offered even finer tools for designing better strategies for protein analysis.<sup>102</sup> Techniques of nano-/micro-fabrication drive the development of digital ELISA,<sup>10</sup> where proteins can be encapsulated and analyzed at a single molecular level. Protein-responsive DNA nanotechnology, such as proximity ligation assays<sup>103,104</sup> and binding-induced DNA assembly,<sup>105,106</sup> allows the development of homogeneous assays for ultrasensitive protein detection without the need for tedious washing steps. Novel biohybrid nanomaterials, with their unique structural, chemical, catalytic, and optical properties, have facilitated the design of better signal transduction or amplification strategies for protein detection and quantification.<sup>16–20</sup>

In this review, we highlighted the emerging roles of nanomaterials for enhancing or replacing conventional enzyme-based signal readout systems in ELISA. Plasmonic or polymeric nanomaterials have been used as substrate-alternatives in ELISA, enabling ultrasensitive visual readouts that are ideal for POCT applications. Diverse nanozymes have been created, which demonstrate comparable or even better enzymatic activities than natural enzymes but are chemically more stable and less sensitive to environmental factors. Non-enzymatic readout systems making use of nanocarriers and DNA nanotechnology have also been adapted to conventional ELISA systems, allowing sensitive and rapid signal amplification with flexible assay designs. These nanomaterial-enhanced immunoassays drastically improve the analytical performance of conventional ELISA without significantly altering the assay format. As such, these technical advances can be rapidly adopted to existing ELISA detection platforms for diverse biological and clinical applications.

To further expand nanomaterial-enhanced immunoassays for real-world applications, several challenges remain to be addressed. First, antibody-based immunoassays are known to be subject to nonspecific adsorption and cross-reactions.<sup>107</sup> Better ligands need to be designed and integrated to nanomaterials for improving assay performance. Synthetic ligands, such as aptamers and molecularly imprinted polymers,<sup>108</sup> are ideal candidates for such applications, as they can be evolved and/or designed for more specific biorecognition than antibodies. Recent advances in structural DNA nanotechnology have enabled the design of multivalent ligands with well-defined spatial distribution.<sup>77–80</sup> Second, most nanomaterial-enhanced readout systems are designed for the detection of a single or limit number of proteins. Multiplexed detection of a panel of protein markers is often necessary for making better clinical decisions. Combining nanomaterials with advanced microfluidic ELISA systems may help address the throughput issue.<sup>109–111</sup> Finally, similar to conventional ELISA, most nanomaterial-enhanced immunoassays are currently developed and validated in the microplate systems. The movement of these assays from laboratory setting to POCT and field-based applications, it is necessary to combine nanomaterial-based readout with miniaturized ELISA platforms, such as those achieved using paper-based microfluidics and portable device fabrication.<sup>112–115</sup>

## Conflicts of interest

There are no conflicts to declare.

## Acknowledgements

The work is supported by the Fundamental Research Funds for the Central Universities, the National Sciences and Engineering Research Council of Canada, and the Ontario Ministry of Research, Innovation and Science.

## Notes and references

- 1 E. Engvall and P. Perlmann, *Immunochemistry*, 1971, **8**, 871–874.
- 2 S. S. Pierangeli and E. N. Harris, *Nat. Protoc.*, 2008, **3**, 840–848.
- 3 L. Asensio, I. González, T. García and R. Martín, *Food Control*, 2008, **19**, 1–8.
- 4 B. M. Beatriz, *et al.*, *Environ. Sci. Technol.*, 2005, **39**, 3896–3903.
- 5 M. F. Clark, R. M. Lister and M. B. Joseph, *Methods Enzymol.*, 1986, **118**, 742–766.
- 6 W. Jongbloed, M. I. Kester, W. M. Flier, R. Veerhuis, P. Scheltens, M. A. Blankenstein and C. E. Teunissen, *Alzheimers Dement.*, 2013, **9**, 276–283.
- 7 V. H. Flood, J. C. Gill, P. A. Morateck, P. A. Christopherson, K. D. Friedman, S. L. Haberichter, R. G. Hoffmann and R. R. Montgomery, *Blood*, 2011, **117**, e67–e74.
- 8 C. S. Thaxton, R. Elghanian, A. D. Thomas, S. I. Stoeva, J.-S. Lee, N. D. Smith, A. J. Schaeffer, H. Klocker, W. Horninger, G. Bartsch and C. A. Mirkin, *Proc. Natl. Acad. Sci. U. S. A.*, 2009, **106**, 18437–18442.
- 9 T. Sano, C. L. Smith and C. R. Cantor, *Science*, 1992, **258**, 120–122.
- 10 D. M. Rissin, *et al.*, *Nat. Biotechnol.*, 2010, **28**, 595–600.
- 11 B. Berg, B. Cortazar, D. Tseng, H. Ozkan, S. Feng, Q. Wei, O. B. Garner and A. Ozcan, *ACS Nano*, 2015, **9**, 7857–7866.
- 12 T. Laksanasopin, T. W. Guo, S. Nayak, A. A. Sridhara, J. E. Justman, S. Nsanjimana and S. K. Sia, *Sci. Transl. Med.*, 2015, **7**, 273re1.
- 13 X. Wu, M. K. K. Oo, K. Reddy, Q. Chen, Y. Sun and X. Fan, *Nat. Commun.*, 2014, **5**, 3779.
- 14 Y. Song, Y. Huang, X. Liu, X. Zhang, M. Ferrari and L. Qin, *Trends Biotechnol.*, 2014, **32**, 132–139.
- 15 D. Q. González and A. Merkoçi, *Chem. Soc. Rev.*, 2018, **47**, 4697–4709.
- 16 S. Song, Y. Qin, Y. He, Q. Huang, C. Fan and H. Y. Chen, *Chem. Soc. Rev.*, 2010, **39**, 4234–4243.
- 17 X. Pei, B. Zhang, J. Tang, B. Liu, W. Lai and D. Tang, *Anal. Chim. Acta*, 2013, **758**, 1–18.
- 18 Y. Zhang, Y. Guo, Y. Xianyu, W. Chen, Y. Zhao and X. Jiang, *Adv. Mater.*, 2013, **25**, 3802–3819.
- 19 X. Yang, Y. Tang, R. R. Alt, X. Xie and F. Li, *Analyst*, 2016, **141**, 3473–3481.
- 20 Z. Farka, T. Juřík, D. Kovář, L. Trnková and P. Skládal, *Chem. Rev.*, 2017, **117**, 9973–10042.
- 21 P. K. Jain, K. S. Lee, I. H. El-Sayed and M. A. El-Sayed, *J. Phys. Chem. B*, 2006, **110**, 7238–7248.
- 22 B. Jiang, D. Duan, L. Gao, G. Nie, M. Liang and X. Yan, *Nat. Protoc.*, 2018, **13**, 1506–1520.
- 23 P. D. Josephy, T. Eling and R. P. Mason, *J. Biol. Chem.*, 1982, **257**, 3669–3675.
- 24 Z. Xuan, M. Li, P. Rong, W. Wang, Y. Li and D. Liu, *Nanoscale*, 2016, **8**, 17271–17277.
- 25 J. Satija, N. Punjabi, D. Mishraac and S. Mukherji, *RSC Adv.*, 2016, **6**, 85440–85456.



- 26 M. Salomón and M. N. Eden, *Front. Bioeng. Biotechnol.*, 2019, **7**, 1–10.
- 27 L. Zheng, G. Cai, S. Wang, M. Liao, Y. Li and J. Lin, *Biosens. Bioelectron.*, 2019, **124–125**, 143–149.
- 28 R. de la Rica and M. M. Stevens, *Nat. Nanotechnol.*, 2012, **7**, 821–824.
- 29 D. Liu, J. Yang, H.-F. Wang, Z. Wang, X. Huang, Z. Wang, G. Niu, A. R. H. Walker and X. Chen, *Anal. Chem.*, 2014, **86**, 5800–5806.
- 30 M. Peng, W. Ma and Y.-T. Long, *Anal. Chem.*, 2015, **87**, 5891–5896.
- 31 D. Liu, Z. Wang, A. Jin, X. Huang, X. Sun, F. Wang, Q. Yan, S. Ge, Ni. Xia, G. Niu, G. Liu, A. R. H. Walker and Xi. Chen, *Angew. Chem., Int. Ed.*, 2013, **52**, 14065–14069.
- 32 X. M. Nie, R. Huang, C. X. Dong, L. J. Tang, R. Gui and J. H. Jiang, *Biosens. Bioelectron.*, 2014, **58**, 314–319.
- 33 Y. Xianyu, Z. Wang and X. Jiang, *ACS Nano*, 2014, **8**, 12741–12747.
- 34 Y. Xianyu, Y. Chen and X. Jiang, *Anal. Chem.*, 2015, **87**, 10688–10692.
- 35 H. Chen, L. Shao, Q. Li and J. Wang, *Chem. Soc. Rev.*, 2013, **42**, 2679–2724.
- 36 H. Liao and J. H. Hafner, *Chem. Mater.*, 2005, **17**, 4636–4641.
- 37 S. A. Alex, N. Chandrasekaran and A. Mukherjee, *Anal. Methods*, 2016, **8**, 2131–2137.
- 38 Y. Li, X. Ma, Z. Xu, M. Liu, Z. Lin, B. Qiu, L. Guo and G. Chena, *Analyst*, 2016, **141**, 2970–2976.
- 39 Y. Lin, S. Xu, J. Yang, Y. Huang, Z. Chen, B. Qiu, Z. Lin, G. Chen and L. Guo, *Sens. Actuators, B*, 2018, **267**, 502–509.
- 40 Z. Gao, K. Deng, X.-D. Wang, M. Miró and D. Tang, *ACS Appl. Mater. Interfaces*, 2014, **6**, 18243–18250.
- 41 X. Ma, Y. Lin, L. Guo, B. Qiu, G. Chen, H. Yang and Z. Lin, *Biosens. Bioelectron.*, 2017, **87**, 122–128.
- 42 J. Li, M. A. Baird, M. A. Davis, W. Tai, L. S. Zweifel, K. M. A. Waldorf, M. Jr, L. Rajagopal, R. H. Pierce and X. Gao, *Nat. Biomed. Eng.*, 2017, **1**, 1–12.
- 43 A. Asati, S. Santra, C. Kaittanis, S. Nath and J. M. Perez, *Angew. Chem., Int. Ed.*, 2009, **48**, 2308–2312.
- 44 W. He, Y. Liu, J. Yuan, J. J. Yin, X. Wu, X. Hu, K. Zhang, J. Liu, C. Chen, Y. Ji and Y. Guo, *Biomaterials*, 2011, **32**, 1139–1147.
- 45 Y. Wana, P. Qia, D. Zhang, J. Wu and Y. Wang, *Biosens. Bioelectron.*, 2012, **33**, 69–74.
- 46 H. Wei and E. Wang, *Chem. Soc. Rev.*, 2013, **42**, 6060–6093.
- 47 L. Z. Gao, J. Zhuang, L. Nie, J. B. Zhang, Y. Zhang, N. Gu, T. H. Wang, J. Feng, D. L. Yang, S. Perrett and X. Yan, *Nat. Nanotechnol.*, 2007, **2**, 577–583.
- 48 D. Duan, K. Fan, D. Zhang, S. Tan, W. Liu, X. Qiu, G. P. Kobinger, G. F. Gao and X. Yan, *Biosens. Bioelectron.*, 2015, **74**, 134–141.
- 49 J. Mu, Y. Wang, M. Zhao and L. Zhang, *Chem. Commun.*, 2012, **48**, 2540–2542.
- 50 C. Zheng, A.-X. Zheng, B. Liu, X.-L. Zhang, Y. He, J. Li, H. H. Yang and G. Chen, *Chem. Commun.*, 2014, **50**, 13103–13106.
- 51 W. Chen, J. Chen, A. L. Liu, L. M. Wang, G. W. Li and X. H. Lin, *ChemCatChem*, 2011, **3**, 1151–1154.
- 52 N. Singh, M. A. Savanur, S. Srivastava, P. D'Silva and G. Mughesh, *Angew. Chem.*, 2017, **129**, 14455–14459.
- 53 H. Ye, K. Yang, J. Tao, Y. Liu, Q. Zhang, S. Habibi, Z. Nie and X. Xia, *ACS Nano*, 2017, **11**, 2052–2059.
- 54 L. Jiao, L. Zhang, W. Du, H. Li, D. Yang and C. Zhu, *Nanoscale*, 2018, **10**, 21893–21897.
- 55 C. N. Loynachan, M. R. Thomas, E. R. Gray, D. A. Richards, J. Kim, B. S. Miller, J. C. Brookes, S. Agarwal, V. Chudasama, R. A. McKendry and M. M. Stevens, *ACS Nano*, 2018, **12**, 279–288.
- 56 X. Zhang, L. Deng, C. Huang, J. Zhang, X. Hou, P. Wu and J. Liu, *Chem. – Eur. J.*, 2018, **24**, 2602–2608.
- 57 C. Penga, M. Hua, N. Li, Y. Hsu, Y. Chen, C. Chuang, S. Pang and H. Yang, *Biosens. Bioelectron.*, 2019, **126**, 581–589.
- 58 Y. Huang, J. Ren and X. Qu, *Chem. Rev.*, 2019, **119**, 4357–4412.
- 59 Z. Zhang, X. Zhang, B. Liu and J. Liu, *J. Am. Chem. Soc.*, 2017, **139**, 5412–5419.
- 60 Z. Zhang, Y. Li, X. Zhang and J. Liu, *Nanoscale*, 2019, **11**, 4854–4863.
- 61 J. Zhang, S. Wu, X. Lu, P. Wu and J. Liu, *Nano Lett.*, 2019, **19**, 3214–3220.
- 62 W. He, Y. Liu, J. Yuan, J. J. Yin, X. Wu, X. Hu, K. Zhang, J. Liu, C. Chen, Y. Ji and Y. Guo, *Biomaterials*, 2011, **32**, 1139–1147.
- 63 W. Zhao, R. Chen, P. Dai, X. Li, J. Xu and H. Chen, *Anal. Chem.*, 2014, **86**, 11513–11516.
- 64 L. Feng, Z. Bian, J. Peng, F. Jiang, G. Yang, Y. Zhu, D. Yang, L. Jiang and J. Zhu, *Anal. Chem.*, 2012, **84**, 7810–7815.
- 65 D. Liu, X. Huang, Z. Wang, A. Jin, X. Sun, L. Zhu, F. Wang, Y. Ma, G. Niu, A. R. H. Walker and X. Chen, *ACS Nano*, 2013, **7**, 5568–5576.
- 66 G. Fu, S. T. Sanjay, M. Doua and X. Li, *Nanoscale*, 2016, **8**, 5422–5427.
- 67 M. Lee, H. Kim, B. Kim, J. Jung and T. Kang, *ACS Appl. Mater. Interfaces*, 2018, **10**, 37829–37834.
- 68 Q. Liu, S. Cheng, R. Chen, J. Ke, Y. Liu, Y. Li, W. Feng and F. Li, *ACS Appl. Mater. Interfaces*, 2020, **12**, 4358–4365.
- 69 J. M. Nam, S. J. Park and C. A. Mirkin, *J. Am. Chem. Soc.*, 2002, **124**, 3820–3821.
- 70 J. M. Nam, C. S. Thaxton and C. A. Mirkin, *Science*, 2003, **301**, 1884–1886.
- 71 M.-P. N. Bui, S. Ahmed and A. Abbas, *Nano Lett.*, 2015, **15**, 6239–6246.
- 72 W. Qu, Y. Liu, D. Liu, Z. Wang and X. Jiang, *Angew. Chem., Int. Ed.*, 2011, **50**, 3442–3445.
- 73 S. Wang, L. Zhang, S. Wan, S. Cansiz, C. Cui, Y. Liu, R. Cai, C. Hong, I. T. Teng, M. Shi, Y. Wu, Y. Dong and W. Tan, *ACS Nano*, 2017, **11**, 3943–3949.

- 74 Y. Lin, J. Jia, R. Yang, D. Chen, J. Wang, F. Luo, L. Guo, B. Qiu and Z. Lin, *Anal. Chem.*, 2019, **91**, 3717–3724.
- 75 J. Wang, C. Xia, L. Yang, Y. Li, C. Li and C. Huang, *Anal. Chem.*, 2020, **92**, 4046–4052.
- 76 N. C. Seeman, *J. Theor. Biol.*, 1982, **99**, 237–247.
- 77 A. R. Chandrasekaran and O. Levchenko, *Chem. Mater.*, 2016, **28**, 5569–5581.
- 78 P. Chidchob and H. F. Sleiman, *Curr. Opin. Chem. Biol.*, 2018, **46**, 63–70.
- 79 Z. Li, J. Wang, Y. Li, X. Liu and Q. Yuan, *Mater. Chem. Front.*, 2018, **2**, 423–436.
- 80 Y. Zhang, J. Tu, D. Wang, H. Zhu, S. K. Maity, X. Qu, B. Bogaert, H. Pei and H. Zhang, *Adv. Mater.*, 2018, **30**, 1–44.
- 81 W. Wang, S. Yu, S. Huang, S. Bi, H. Han, J. Zhang, Y. Lu and J. Zhu, *Chem. Soc. Rev.*, 2019, **48**, 4892–4920.
- 82 S. D. Mason, Y. Tang, Y. Li, X. Xie and F. Li, *Trends Anal. Chem.*, 2018, **107**, 212–221.
- 83 L. Yuan, M. Giovanni, J. Xie, C. Fan and D. T. Leong, *NPG Asia Mater.*, 2014, **6**, e1120.
- 84 Z. Li, B. Zhao, D. Wang, Y. Wen, G. Liu, H. Dong, S. Song and C. Fan, *ACS Appl. Mater. Interfaces*, 2014, **6**, 17944–17953.
- 85 X. Liu, Y. Xu, T. Yu, C. Clifford, Y. Liu, H. Yan and Y. Chang, *Nano Lett.*, 2012, **12**, 4254–4259.
- 86 N. R. Sundah, N. R. Y. Ho, G. S. Lim, A. Natalia, C. W. Chan, T. P. Loh and H. Shao, *Nat. Biomed. Eng.*, 2019, **3**, 684–694.
- 87 P. S. Kwon, S. Ren, S. Kwon, R. J. Linhardt, J. Chao and X. Wang, *Nat. Chem.*, 2020, **12**, 26–35.
- 88 Y. Zhao, F. Chen, Q. Li, L. Wang and C. Fan, *Chem. Rev.*, 2015, **115**, 12491–12545.
- 89 C. Jung and A. D. Ellington, *Acc. Chem. Res.*, 2014, **47**, 1825–1835.
- 90 Y. Tang, Y. Lin, X. Yang, Z. Wang, X. C. Le and F. Li, *Anal. Chem.*, 2015, **87**, 8063–8066.
- 91 H. Zhang, F. Li, B. Dever, X.-F. Li and X. C. Le, *Chem. Rev.*, 2013, **113**, 2812–2841.
- 92 S. Bi, S. Yue and S. Zhang, *Chem. Soc. Rev.*, 2017, **46**, 4281–4298.
- 93 J. Choi, K. R. Love, Y. Gong, T. M. Gierahn and J. C. Love, *Anal. Chem.*, 2011, **83**, 6890–6895.
- 94 R. Lin, Q. Feng, P. Li, P. Zhou, R. Wang, Z. Liu, Z. Wang, X. Qi, N. Tang, F. Shao and M. Luo, *Nat. Methods*, 2018, **15**, 275–278.
- 95 B. Zhang, B. Liu, D. Tang, R. Niessner, G. Chen and D. Knopp, *Anal. Chem.*, 2012, **84**, 5392–5399.
- 96 L. Hou, X. Wu, G. Chen, H. Yang, M. Lu and D. Tang, *Biosens. Bioelectron.*, 2015, **68**, 487–493.
- 97 W. Zhuang, Y. Li, J. Chen, W. Liua and H. Huang, *Anal. Methods*, 2019, **11**, 2597–2604.
- 98 Y. Zhao, S. Hu, H. Wang, K. Yu, Y. Guan, X. Liu, N. Li and F. Liu, *Anal. Chem.*, 2017, **89**, 6907–6914.
- 99 G. Wang, L. Chen, X. He, Y. Zhu and X. Zhang, *Analyst*, 2014, **139**, 3895–3900.
- 100 Y. Lv, R. Peng, Y. Zhou, X. Zhang and W. Tan, *Chem. Commun.*, 2016, **52**, 1413–1415.
- 101 M. Gao, F. He, B. Yin and B. Ye, *Analyst*, 2019, **144**, 1995–2002.
- 102 Z. Farka, T. Jurik, D. Kovar, L. Trnkova and P. Skladal, *Chem. Rev.*, 2017, **117**, 9973–10042.
- 103 S. Fredriksson, M. Gullberg, J. Jarvius, C. Olsson, K. Pietras, S. M. Gustafsdottir, A. Ostman and U. Landegren, *Nat. Biotechnol.*, 2002, **20**, 473–477.
- 104 F. Li, H. Zhang, C. Lai, X.-F. Li and X. C. Le, *Angew. Chem., Int. Ed.*, 2012, **51**, 9317–9320.
- 105 F. Li, H. Zhang, Z. Wang, X. Li, X.-F. Li and X. C. Le, *J. Am. Chem. Soc.*, 2013, **135**, 2443–2446.
- 106 F. Li, Y. Lin and X. C. Le, *Anal. Chem.*, 2013, **85**, 10835–10841.
- 107 D. A. Giljohann and C. A. Mirkin, *Nature*, 2009, **462**, 461–464.
- 108 F. Li, H. Zhang, Z. Wang, M. A. Newbigging, S. M. Reid, X.-F. Li and X. C. Le, *Anal. Chem.*, 2015, **87**, 274–292.
- 109 A. H. C. Ng, R. Fobel, C. Fobel, J. Lamanna, D. G. Rackus, E. Lam and A. R. Wheeler, *Sci. Transl. Med.*, 2018, **10**, eaar6067.
- 110 C. Liu, X. Xu, B. Li, B. Situ, W. Pan, Y. Hu, T. An, S. Yao and L. Zheng, *Nano Lett.*, 2018, **18**, 4226–4232.
- 111 C. Dixon, A. H. C. Ng, R. Fobel, M. B. Miltenburg and A. R. Wheeler, *Lab Chip*, 2016, **16**, 4560–4568.
- 112 J. Liu, Z. Geng, Z. Fan, J. Liu and H. Chen, *Biosens. Bioelectron.*, 2019, **132**, 17–37.
- 113 M. M. Gong and D. Sinton, *Chem. Rev.*, 2017, **117**, 8447–8480.
- 114 L. Soleymani and F. Li, *ACS Sens.*, 2017, **2**, 458–467.
- 115 L. Syedmoradi, M. Daneshpour, M. Alvandipour, F. A. Gomez, H. Hajghassem and K. Omidfar, *Biosens. Bioelectron.*, 2017, **87**, 373–387.